

# Recent Advances in Research on Solid Rocket Propulsion

Y. Fabignon, J. Anthoine,  
D. Davidenko, R. Devillers,  
J. Dupays, D. Gueyffier,  
J. Hijlkema, N. Lupoglazoff,  
J. M. Lamet, L. Tessé, A. Guy,  
C. Erades  
(ONERA)

E-mail : yves.fabignon@onera.fr

DOI : 10.12762/2016.AL11-13

This paper is devoted to a review of some recent studies conducted at ONERA within the framework of solid rocket propulsion for missiles, as well as space launchers. The viewpoint adopted is to present the physical phenomena studied using modeling, simulations and experimentations. Three major scientific topics will be investigated in this article: combustion of solid propellants; motor interior ballistics with a focus on two-phase flows, turbulence and radiative effects; rocket exhaust plumes, including phenomena in the vicinity of the aft body.

## Introduction

Solid Rocket Motors (SRM) serve as the propulsion back-bone for strategic and tactical missiles, as well as space launchers. Since most missions do not require the sophistication of multiple restart and throttling operations, solid propulsion becomes an interesting choice because of its inherent safety, reliability, simplicity, high density impulse, minimum maintenance, and low cost. The configuration of a rocket motor has to be designed to meet requirements or operational conditions, depending on the mission. The combustion of solid propellant controls the operational conditions of a SRM through the burn rate versus the chamber pressure and temperature sensitivity. The understanding of the combustion mechanisms of solid propellants is therefore an important field of interest for the solid grain designer. A section dedicated to this topic is presented in this article, with a focus on numerical approaches to study the combustion of solid propellants.

The addition of aluminum powder in the propellant improves SRM thrust performance, but leads to the formation of liquid aluminum oxide droplets and therefore produces a two-phase flow in the chamber. This two-phase flow can impact pressure oscillations and may lead to some issues, such as slag accumulation, nozzle erosion, two-phase losses, and so on. The main physical phenomena at the origin of the two-phase flow in the rocket chamber are presented in a second section of this article. Experimental and numerical approaches are also discussed.

Turbulence can play a significant role in the motor chamber and its prediction remains a difficult task, due to the flow induced by mass injection from the propellant surface. Extensive experimental works on cold flows with surface transpiration were carried out in the past, in order to represent the flow in the motor chamber. Results showed the transition to turbulence and the coupling with acoustics.

Numerical simulations have been performed to study the flow field in a motor chamber using RANS approaches and, more recently, LES of nonreacting flows. Still today, it turns out that modeling the transition to turbulence inside an actual SRM is a challenging task. A section of this article is devoted to this difficult problem, using recent advances in High Performance Computing (HPC).

Metalized solid propellants have higher final flame temperatures and therefore higher radiant intensities than non-metalized propellants. The importance of radiative heat feedback on the propellant surface, in case of the combustion of metalized propellants, is often ignored by researchers and can lead to discrepancies in the measured and predicted gas temperatures. A short review on radiative effects in the rocket chamber is presented in a section of this article, with some applications using numerical simulations.

The last topic discussed in this article concerns phenomena in the vicinity of the aft body of solid rocket motors and their exhaust plumes. In the first part of this section, we describe an experimental setup, in order to validate numerical simulations in the base region of a solid rocket motor with an external flow field. The second part is devoted to the simulation of exhaust plumes motivated by the need of predicting infrared and radar signatures.

Within the framework of space launchers, large SRMs are used and are subject to pressure and thrust oscillations whose origin relies on the coupling between hydrodynamic instabilities and the first longitudinal acoustic modes of the combustion chamber. ONERA, in collaboration with SAFRAN/HERAKLES and CNES, has investigated this physical phenomenon thoroughly over the last two decades [1, 2].

In particular, small scale firing tests, numerical simulations and application of the linear stability theory were performed to better understand the mechanism of pressure oscillations and to propose practical solutions, in order to remove them, or at least reduce them [3-6]. This section will not be further described in the paper, but the reader can refer to the listed references for more details.

## Combustion of solid propellants

Ammonium Perchlorate (AP) and a binder, such as polybutadiene, are the main ingredients in propellants used in major operational SRMs. The combustion of AP results in a premixed flame at about 1  $\mu\text{m}$  from the surface, at roughly 1200 K or higher. Combustion modeling of this energetic ingredient has been the subject of numerous investigations over last decades, but only some researchers have described the flame structure accurately. The methodology used at ONERA to calculate the AP flame structure is to consider a one-dimensional model, taking into account a detailed gas-phase chemistry with 36 species and 216 reactions [7]. The corresponding nonlinear system of differential equations is numerically solved by using adaptive continuation techniques [8]. One of the new results from the model is the structure of the temperature profile (Figure 1). For usual operating pressure, there are two maxima: the first one ( $\approx 1300$  K) is due to the AP premixed flame while the second maximum ( $\approx 1400$  K) corresponds to the equilibrium temperature. The multi-scale character of the combustion is due to the slow kinetics of nitrogen-based components modifying the flame structure.

Steady-state sensitivity parameters, namely pressure and initial temperature sensitivities of the burning rate and surface temperature, are also numerically obtained [9]. For an intrinsically stable combustion, the Zel'dovich-Novozhilov or (ZN) [10] response function can be calculated, using steady-state sensitivity parameters. For solid propellants, the response function  $R_p$  is defined as follows:

$$R_p = \frac{m' / \bar{m}}{p' / \bar{p}}$$

Where  $\bar{m}$  and  $\bar{p}$  are respectively the steady-state mass flow rate and pressure at the propellant surface, and  $m'$  and  $p'$  are the corresponding unsteady fluctuations. The response function is a linear

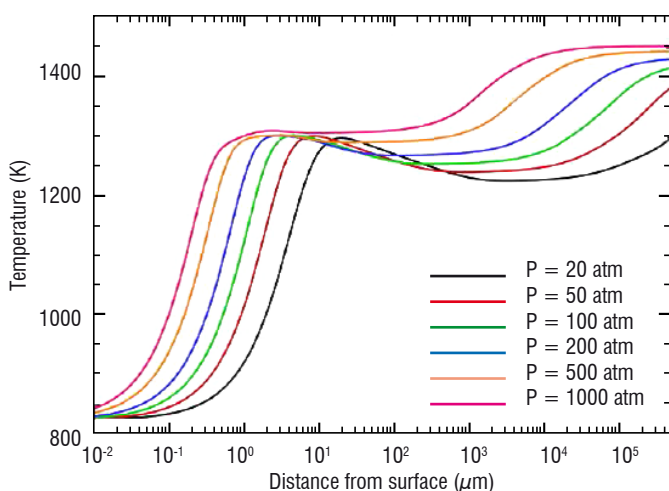


Figure 1 - AP flame structure at different pressures

representation of the coupling between acoustics and combustion. It is an important parameter in the analysis of SRM instabilities [11]. For AP the real part of the ZN response function (Figure 2) has been compared with the data of Finlinton *et al* [12]. Beyond the linear approach, the model developed has been used to study acoustic/elastic wave propagation. It has been shown [13] that the interface between the gas and solid phases can reflect back a wave of the same frequency as the incident wave. In the particular case used, the classical linear response function can be affected [14].

As mentioned above, composite propellants in major operational SRMs consist of oxidizer particles (AP) embedded in a polybutadiene; therefore, they are heterogeneous at the scale of the oxidizer particles. Consecutively, the burning rate is influenced by the propellant morphology and the size distribution of the oxidizer particles. In the previous decade, we tried to calculate the burning rate of the heterogeneous propellant by using a method based on the averaging of the component burning rates. It turned out that this method was not accurate and required much experimental data for validation. Any serious attempt to simulate the propellant burning rate numerically must incorporate an adequate representation of its microstructure by random packing. This realistic approach was developed and used in many modeling studies [15-17]. At ONERA, the modeling approach based on random packing representation of composite propellants has been also investigated. Here, some results are presented to demonstrate the application of the main modeling tools. The reader can find more details in the recent publication [18].

Generation of random particle packs must satisfy the necessary requirements for a high packing density, a wide particle size distribution, and a large number of particles. At present, two packing methods for multidisperse spherical particles have been realized in efficient numerical tools. One of these methods, based on Lubachevsky's algorithm, processes a system of randomly moving particles whose size grows in time. Being computationally expensive, this method can produce very dense random packs close to the jamming limit when the particles have no room to move. Another method is based on the Random Sequential Adsorption (RSA) algorithm, which is much less expensive but results in packs of relatively low density. For the first time, we used the RSA method to generate propellant packs with realistic granulometry and demonstrated that it is capable of producing model packs with the desired density. As an illustration, a 3D

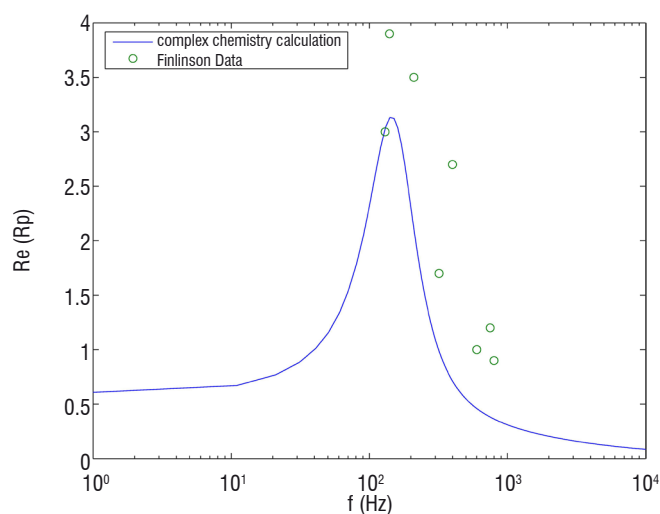


Figure 2 - Real part of ZN response function and comparison with the data of Finlinton *et al* [12]

random pack of  $10^5$  AP particles, generated with the RSA method, is shown in Figure 3. It is composed of 38 particle classes with a real size distribution. The packing density is 77%, which corresponds to a real propellant.

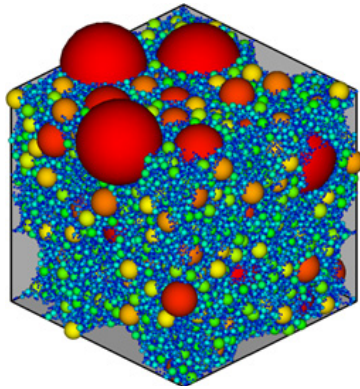


Figure 3 - Random pack of  $10^5$  AP particles in a cubic periodic domain. Colors correspond to different particle classes

Heat transfer modeling in composite propellants requires specific care, because of very different thermophysical properties of the propellant components and a wide range of geometrical scales. A specific approach, based on the finite-volume method, has been developed for propellants composed of AP and aluminum particles in a HTPB binder. We have focused on minimizing the numerical error due to the material structure discretization on a Cartesian mesh. Computational results obtained for an AP-HTPB sample under steady-state heat transfer are presented in Figure 4, which shows 2D and 3D maps of relative non-uniformity of the temperature field in a mid-section of the sample.

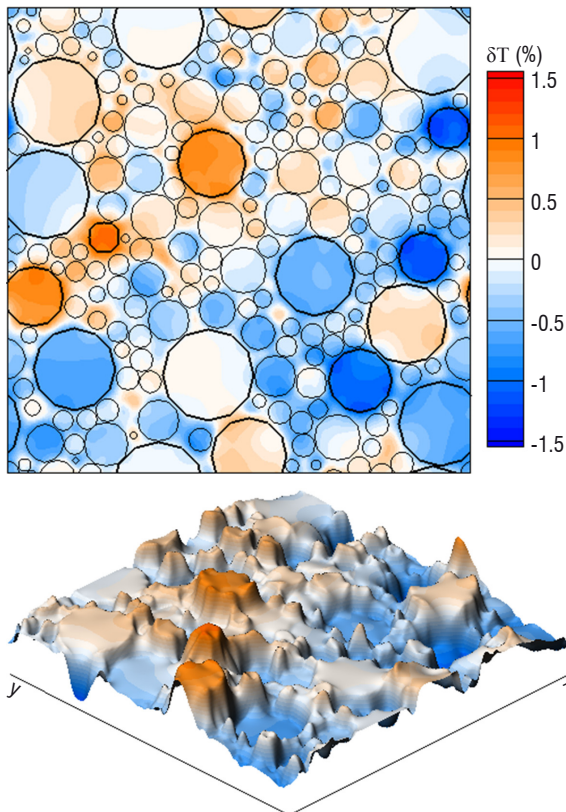


Figure 4 - Temperature non-uniformity in an AP-HTPB sample under steady-state heat transfer. 2D map on the top and 3D on the bottom

Correct prediction of the temperature field in the solid propellant is very important for combustion modeling that requires a coupled treatment of physico-chemical processes in the solid propellant and the hot gas of combustion products. In order to simulate the gas flow, a Navier-Stokes solver for a multispecies reacting gas has been developed according to the low-Mach formulation. The numerical solution for the solid and gas phases is sought on a common Cartesian mesh and coupled by some interface conditions on the regression surface. The propellant surface regression is governed by pyrolysis laws for each ingredient and strongly depends on the local temperature, thus the regression surface features a rather complex geometry and motion. It is treated by the level set method suitable for any arbitrary shape and topology of the regression surface. A level set simulation of the regression of a 3D sample is illustrated in Figure 5. The regression speed is specified as a function of the material composition. Being initially planar, the regression surface evolves to an irregular shape, due to the sample random structure. Another illustration is shown in Figure 6 for the combustion of a 2D AP-HTPB sample. The propellant composition is visualized in the solid zone and the field of combustion product fractions in the fluid zone. Oxygen-rich product P1 is generated in flame fronts near the AP particles (blue zones), then it reacts with fuel-rich gases from HTPB pyrolysis to produce a final product P2 in diffusion flames (red zones). These results demonstrate that the propellant flame has a multifront structure that constantly evolves over time.

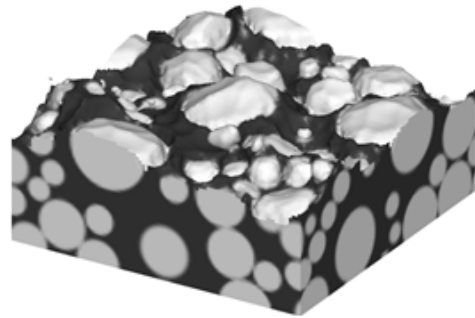


Figure 5 - Simulation of regression surface motion in a 3D sample by the level set method. Regression surface on the top

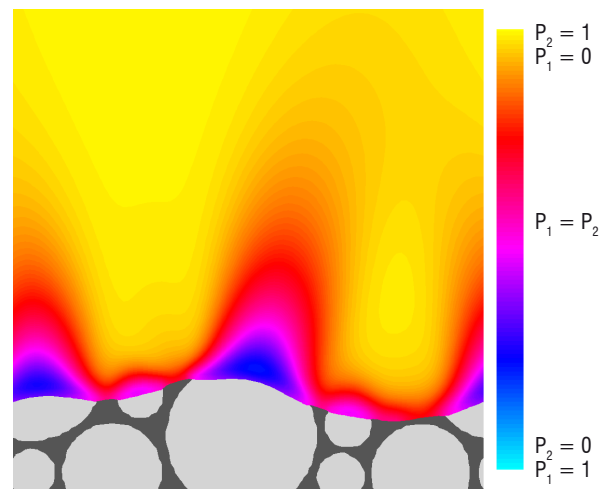


Figure 6 - Combustion simulation with a 2D AP-HTPB sample. Propellant structure and field of combustion product fractions of AP ( $P_1$ ) and HTPB ( $P_2$ )

## Two-phase flows due to aluminum particles

Aluminum powder is generally introduced into the propellant in a significant proportion to increase the flame temperature and thus the motor performance. However, the expected gain is lowered by the presence of a massive amount, often exceeding 30% by weight, of aluminum oxide residues and smoke in the combustion products.

This condensed phase increases the rocket exhaust plume emission and tends to reduce the ejection gas velocity through the drag effect in the expanding nozzle. The resulting so-called "two-phase losses" are generally the main contribution of the total performance loss that affects nozzle efficiency [19], [20]. Inside the motor, these droplets are the source of slag material that may remain in the motor during firing and thereby cause additional performance loss and excessive heating, leading to subsequent insulation erosion where they collect [21]. In addition, aluminum combustion, distributed above the propellant surface, and aluminum oxide behavior in the whole chamber, can also affect combustion instabilities by acting as driving or damping mechanisms through very complex interactions with acoustic waves and various transient or unsteady processes occurring in the confined volume of the chamber [21-24]. Detailed knowledge of condensed phase characteristics and behavior in the motor and the plume are essential to improve motor performance and stability predictions, and also the plume emission estimate.

Experimental and numerical approaches are combined to evaluate the impact of the condensed phase in solid propulsion. Experiments give input data for numerical models or some convenient validation cases, to test both the models and the numerical strategy. They are often conducted with a small to moderate sample of propellant and operated with various measuring, collecting, analyzing and visualization devices. Initial aluminum droplet and residue size distributions, droplet burning time, droplet initial motion characteristics and particle-size distribution in the plume are some examples of useful input or validation data collected from dedicated experiments. For instance, a nephelometer is used for determining the size distribution in the plume from angular static light-scattering measurements [25]. Characteristics of particles in a motor environment are obtained by using two dedicated setups described in the following sections.

The analysis of particles above the surface of burning propellant samples is conducted by using a focusing shadowgraphy setup [26] that enables particle visualization at a high repetition rate (Figure 7). Small propellant samples are tested under a nitrogen atmosphere up to 4 MPa. At higher pressure, smoke is too dense to determine the contours of particles. Propellant ignition is obtained via a high-power laser beam, so that the imaged area remains undisturbed by other ignition species. The hot combustion gases, close to the burning surface, are imaged at repetition rates of up to

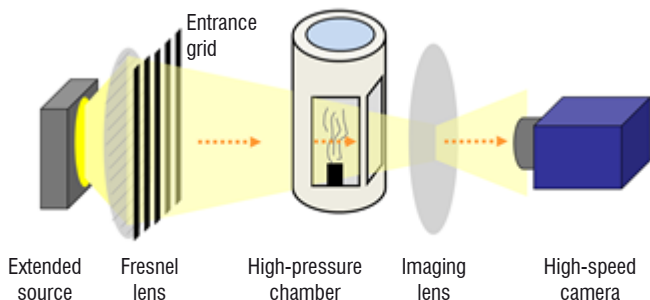


Figure 7 - Experimental shadowgraphy setup used to visualize particles above the propellant surface

10 kHz, with spatial resolutions making it possible to detect particles as small as 10  $\mu\text{m}$ . Hence, common aluminum particles in the range of 20 to 200  $\mu\text{m}$  are well resolved and followed in their vertical movement away from the surface, as seen in the experimental image samples (Figure 8).

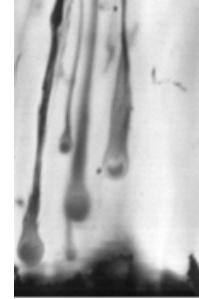


Figure 8 - Shadowgraphy images of aluminum particles leaving the surface of burning propellants

The experimental images are analyzed with automatic image processing tools, to detect and characterize the particles. Automatic scripts are necessary, since  $10^3$  to  $10^4$  images can be acquired during a typical combustion test, each of them showing several dozens of aluminum particles. The main parameters of interest are particle size distributions and velocity distributions, both of which are crucial input parameters for two-phase flow simulations from solid propellant combustion. The analysis process is first validated with research propellants seeded with inert particles [27], because the size of inert particles is well characterized. Other aspects are also being investigated, such as the detailed morphological characterization of burning aluminum droplets, like the ones shown also in Figure 8. Morphological characterization is a way to validate various physical assumptions underlying the aluminum-combustion models used in the numerical codes.

The size distribution of aluminum oxide residues and smoke present in the combustion products is obtained with the so-called KeRC setup (Figure 9), developed by the Russian Keldysh Research Center. It allows for the isokinetic sampling, controlled cooling and capture of liquid aluminum oxide droplets inside a solid propellant motor. Details of the conception, validation and error assessment of the operating method can be found in [28].

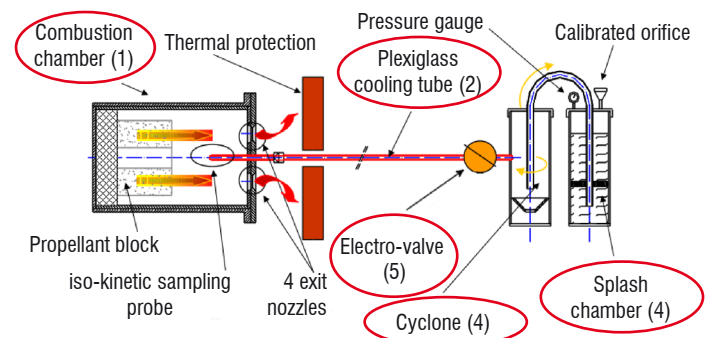


Figure 9 - KeRC experimental setup

The first validation runs of the KeRC setup with a propellant seeded with calibrated, inert particles yielded a systematic bias in favor of the bigger particles. CFD has shown that large vortices at the edge of the cylindrical block deflect smaller particles away from the axis. Replacing the cylindrical grain with a grain without particles and adding a small sample in the center of the block confirmed this hypothesis and improved the measured size distribution. However, the small number of particles in the flow increased the influence of pollutants generated as a by-product of the combustion process. The simulations of the inert experiments have confirmed the potential of the ONERA simulation code CEDRE [29] to correctly reconstruct the internal flow of the KeRC setup. In order to overcome the experimental bias, an "inverse" CFD approach with liquid particles including coalescence and break-up modeling has been developed. By modifying the size distribution of the particles injected at the surface of the grain, based on the comparison of the size distribution of the particles entering the sample probe with the experimental results, we can hope to find a realistic representation of the particles as they leave the surface of the burning propellant grain. Figure 10 shows an illustration of simulation results on a two-phase flow in a typical sampling experiment and a comparison of the experimental and simulated particle size distributions [28]. We numerically inject a bi-modal distribution of particles with mean diameters of  $1\mu\text{m}$  and  $15\mu\text{m}$  and we find a distribution very close to the experimental results inside the sampling probe.

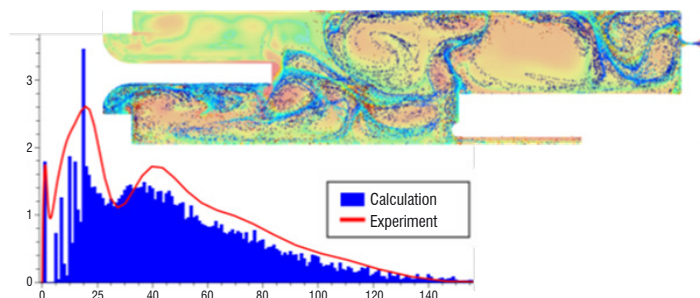


Figure 10 - CEDRE simulations of a typical KeRC experiment

and break-up models, in addition to classical gas-droplet interaction models [30]. Figure 11 shows an example of a simulation performed with the Eulerian sectional approach on an unsteady segmented motor configuration subject to parietal vortex shedding [31]. This approach is based on a piecewise continuous modeling of the particle size distribution defined in a fixed interval (or section) [31, 32]. Such an approach offers in particular a rigorous formalism to manage coalescence and break-up models. Three sections are defined for the simulation, shown in Figure 11, and particles are supposed to be inert so that the size variation is due only to particle-particle interactions.

## Turbulence in the chamber

Flow evolution in a porous duct with surface mass injection resembles the flowfield ensuing from the burning of solid propellant in a rocket motor. The analysis of the transition to turbulence with appreciable fluid injection through a permeable duct has been studied in the past [33], as well as more recently [34]. Results showed that the transition of the mean axial velocity profiles occurs farther downstream in the fully developed turbulent flowfield.

Modeling the transition to turbulence inside an actual SRM is a challenging task, because complex geometries and more physical flows must be taken into account. Any serious attempt to simulate the transition to turbulence in a motor chamber must use an unsteady compressible Navier-Stokes approach, in order to study the effect of Mach number on the turbulence and interactions of acoustic waves with turbulent eddies at a fundamental level.

The CEDRE code [29], developed at ONERA for various applications in the field of energetics, has been used for this task. Its generality and its multiphysics capabilities are greatly appreciated for LES or MILES simulations of SRM internal flows. The experimental setup "c1xb" used (Figure 12) is a small SRM chamber that was designed to develop a vortex shedding phenomenon locked on the first axial mode,

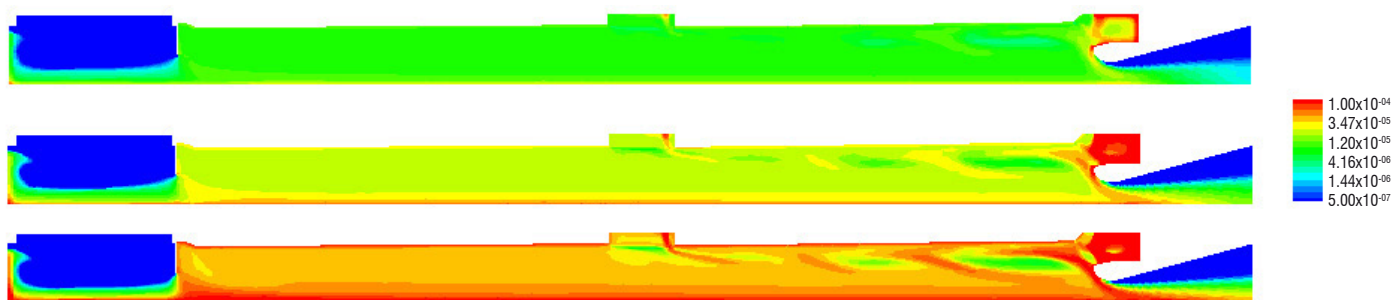


Figure 11 - Particle volume fraction per section (top to bottom: from smaller to larger particles) in the chamber of a segmented motor subject to parietal vortex shedding.

Reliable predictions of the impact of the condensed phase by numerical means need a correct assessment of the complex interactions occurring between the gas and the particles, and between the particles themselves. Together with the particle mass loading, the particle size is a key parameter to correctly reproduce these interactions. The modeling must be able to describe the initial polydisperse particle size distribution and its subsequent evolutions throughout the chamber and the nozzle resulting from interactions with the flow and from particle-particle interactions. Both Lagrangian and Eulerian approaches, available in the CEDRE code, are used with dedicated coalescence

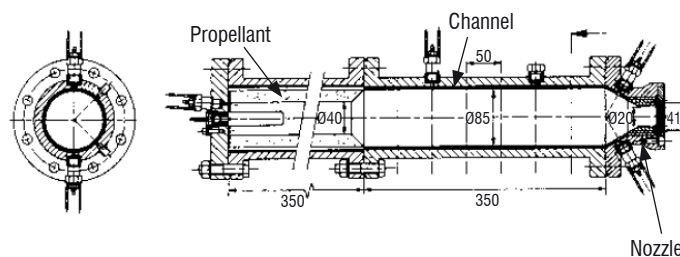


Figure 12 - Schematic diagram of the experimental setup "c1xb" (dim in mm)

as observed in some large SRMs. In the setup, the vortex roll comes from the destabilization of the shear layer generated from a chamfered edge of the propellant. This geometrical singularity is located in the middle of the chamber, to focus the coupling between the vortex roll and the acoustics of the chamber on the first axial mode [35].

All tests experienced pressure oscillations with some bursts corresponding to a sustained self-excitation phenomenon [36]. 2D computations were performed in the past corresponding to several burn times. They have given different vortex shedding frequencies, which were found to correspond to the experimental results [37, 38]. It was noticed that the agreement was good after half-combustion. However, the absence of pressure oscillations during the first half of the combustion could not be explained by 2D computations. The transition to turbulence was suspected to interact with the acoustics.

Recently, with the advent of HPC, a large simulation of the transition to turbulence has been launched within the framework of a GENCI project. The feasibility of a computation in the experimental setup "c1xb", using a mesh of over a billion cells, has been carried out. The initial grain (corresponding to 0 mm burnt) geometry has been chosen for computations, because the flow field should be in transition to turbulence. Gases are injected from both the cylindrical and chamfered parts of the grain, as in the experiments. Four levels of mesh refinements have been considered (Table 1). The CEDRE code was installed on CINES' Occigen, a new massively parallel machine using Haswell processors. A million hours were allocated for computations. Results are shown in Figure 13 for grids 2GG, GM and GF in terms of the so-called Q criterion. One can see that the position of the transition to turbulence is clearly modified between the fine mesh GF and the coarse mesh 2GG. Small turbulent structures are described with the fine mesh GF. The turbulent structures are larger in the case of the mesh 2GG.

Mesh	Number of cells	Number of processors
GG	276 480	64
2GG	6 259 959	256
GM	97 130 691	1008
GF	1 046 185 757	2016 to 4080

Table 1 - Meshes used in the "c1xb" setup and number of processors on the CINES-Occigen supercomputer

An estimation of the Kolmogorov scale  $\eta$  has been performed for the 2GG, GM and GF meshes. Figure 14 shows the ratio of the local grid size  $\Delta$  divided by the Kolmogorov scale  $\eta$ .

A billion cells (GF mesh) enable convergence to nearly a DNS, because the grid size is approximately five times larger than the Kolmogorov scale. In this SRM, we have estimated that a mesh with 100 billion cells would be necessary for a DNS calculation. Such an approach offers new insights for the study of complex flows in SRMs.

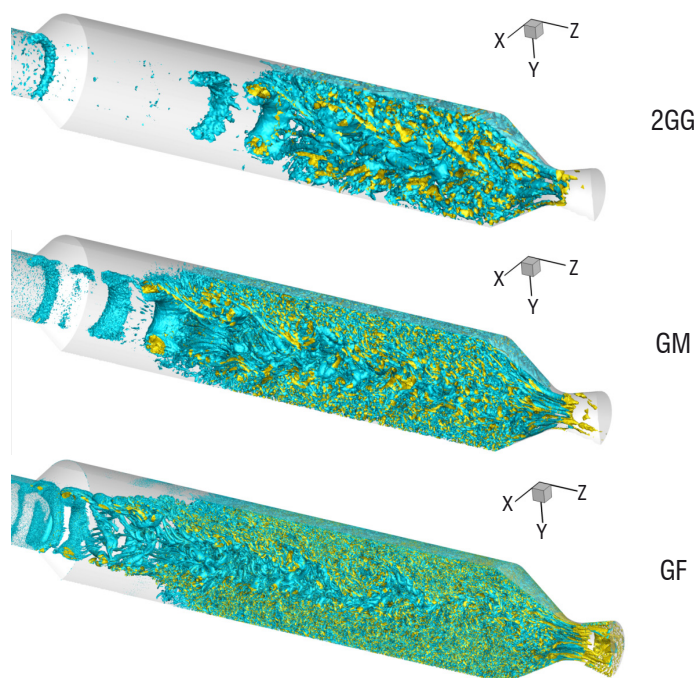


Figure 13 - Snapshots of Q criterion isosurfaces for three different meshes (GF, GM, 2GG)

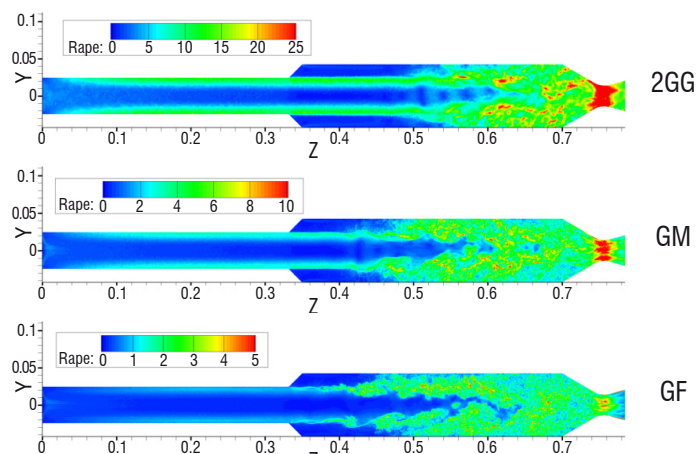


Figure 14 - Snapshots of the ratio  $\Delta / \eta$

## Radiative effects in the chamber

Hot gas and a particle mixture generated by the combustion of an aluminized AP-HTPB propellant is a semi-transparent medium that emits, absorbs and scatters radiation. Usually, four gaseous species are taken into account to compute radiative transfer in a SRM:  $H_2O$ ,  $CO_2$ ,  $CO$  and  $HCl$  [39, 40]. Moreover, in an aluminized solid propellant, the contribution of alumina droplets is generally higher than in a gas propellant. Temperatures of up to 3600 K and a pressure of between 3 to 15 MPa are reached in the combustion chamber, leading to an optically thick medium. A typical extinction length value is about 1 mm [39]. Due to this small value of typical extinction length, wall radiative fluxes strongly depend on the temperature, volume fraction and particle size profiles in the boundary layer.

Two numerical methods have been developed at ONERA: the Discrete Ordinates Method (DOM) in the REA solver [40, 41] and the Monte Carlo Method (MCM) in the ASTRE code [41-46]. The first method offers a good compromise between accuracy and CPU time, but it solves only the differential form of the Radiative Transfer Equation (RTE), with a gas radiative property model necessarily formulated in terms of the absorption coefficient. Moreover, its use requires some assumptions about physical phenomenon modeling (for example, it is impossible to take the turbulence-radiation interaction or spectral correlations rigorously into account when reflecting walls or scattering particles are present). The MCM is a statistical approach that can be used to solve any kind of problem, since it solves the integral form of the RTE, enabling the use of both types of gas radiative property models formulated in terms of the absorption coefficient and transmissivity. Given that the MCM is statistical, exact results can be approximated if enough events are simulated. That is why results obtained with MCM are often considered as reference solutions. Another advantage of MCM is that even the most complicated problem can be solved with minimum assumptions. However, this statistical method is known to converge slowly.

The DOM is based on a discrete representation of the directional variation of the radiative intensity. Thus, the differential form of the RTE is replaced by a system of partial differential equations (one equation for each ordinate direction) and integrals over a range of solid angles are approximated by weighted sums over the ordinate directions within that range. Gaussian quadratures, called level symmetric or  $S_N$  quadratures, are often used. That is why DOM is also called the  $S_N$  method.  $N$  is an even number that indicates the order of the solution. In a three-dimensional problem,  $N(N+2)$  discrete ordinate directions are considered. The REA parallelization is carried out by mesh splitting: each core deals with a piece of the whole computational domain.

MCM consists in following a large number of energy bundles (discrete amounts of energy, which can be pictured as a group of photons bound together) throughout their transport histories, from emission to absorption. Bundle characteristics, namely wave number, initial direction and emission point, and physical events (scattering, reflection of walls, etc., except absorption) along bundle trajectories are chosen according to probability distributions, by drawing random numbers. The absorption phenomenon is treated with the pathlength method, also called energy partitioning, which consists in computing the exponential absorption along the path. Therefore, a bundle contributes to every cell that it traverses. It is traced until it either leaves the computational domain, or until its energy is depleted below a given cut-off level. Since all of the bundles are statistically independent, the parallelization is achieved by distributing them over the processor cores.

As well as the conventional Forward Method (FM), various reciprocal methods, based on the exchange formulation of radiative transfer, are implemented in ASTRE [42-44]: the Emission, Absorption and Optimized Reciprocity Methods, ERM, ARM and ORM, respectively. Reciprocal methods converge faster than FM in optically thick media, like a solid propellant rocket motor [42-44]. Moreover, ERM is very useful to compute only radiative fluxes on selected walls [43, 44].

Due to high pressure in the combustion chamber, radiative transfer can be calculated without taking into account gas spectral correlations. Indeed, at a high pressure, due to the collision broadening effect, the gas absorption spectra display smoother spectral dynamics than those at atmospheric pressure [41]. In this case, the spectral correlation effect is weak and the box model can be used to model the gas radiative properties. Such an approach has been used by Duval [39, 47] or Joumani [40].

In the REA solver, to compute the absorption coefficients of the gaseous mixture, the parameters generated by Duval *et al* [47] are used. These parameters have been tabulated for 43 spectral bands in the infrared spectral range ( $1\ \mu\text{m} - 73\ \mu\text{m}$ ) and for 14 temperatures between 300 K and 2900 K. For upper temperatures, parameters at 2900 K are used.

In the ASTRE code, the same model parameters can be used. Moreover, the updated Statistical Narrow Band (SNB) model parameters, generated by Rivière and Soufiani [48], are also available. In ASTRE, this SNB model can be used in its complete form (formulated in terms of transmissivity [46]) or combined with the weak absorption approximation. This second approach is equivalent to the box model [39, 41]. Indeed, the weak absorption approximation is, for example, valid when pressure is high.

## Particle radiative property modeling

Concerning the particles, only alumina droplets are considered in our simulations. They are assumed to be spherical, homogeneous and isothermal. In a first approximation, aluminum particles are not taken into account in radiative transfer calculations. Then, the Mie theory is applied to compute radiative properties [41]: absorption and scattering coefficients and phase function. The alumina complex refraction index  $m$  is modeled as a function of wavelength  $\lambda$  and temperature  $T$ , in accordance with the expression given by Dombrovsky [49]. Alumina droplets can be in thermal non-equilibrium with the gases, if particle temperatures are calculated by a solver for the dispersed phase.

Moreover, to compute particle radiative properties, a particle size distribution is needed [41]. Two approaches are possible. The particle size distribution can be either calculated by a solver for the dispersed phase, based on a sectional approach, or approximated by several particle classes. From one to five classes are typically considered. For each class, a Gaussian function, centered around a chosen mean diameter with a relative standard deviation of 10 %, is used to model the size distribution.

## Examples of radiative effects

Radiation plays a significant role in SRMs with aluminized propellant. In order to protect the structural parts of the motor, several types of thermal protecting materials are used. The prediction of convective and radiative fluxes on these materials is important, since the flux levels directly affect performance (ablation in the nozzle throat, impulse to weight ratio) and the safety of the motor. The flux levels may be of the order of several  $\text{MW}\cdot\text{m}^{-2}$  and radiative contributions range from practically 100% (internal parts) to about 10% (divergent part of the nozzle). Moreover, it has been shown that radiative fluxes have a strong effect on the ignition of a SRM, due to the radiative heat feedback on the propellant surface, which is a significant fraction of the total heat feedback.

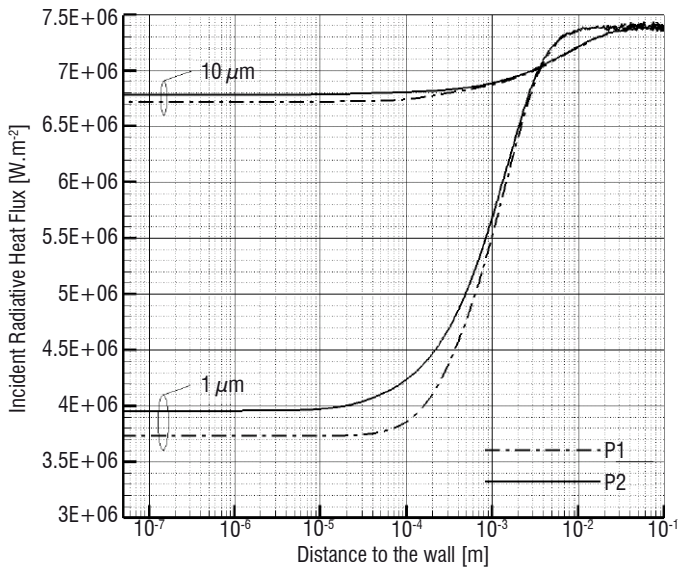


Figure 15 - Incident radiative heat flux as a function of distance to the burning surface [50]

For example, a recent study [50] shows that, for AP/HTPB composite propellants with 17% of aluminum, the radiative flux contribution to the total heat flux on the propellant surface varies from 10% to 25%. Incident radiative heat flux to the burning surface as a function of distance to the propellant surface is illustrated in Figure 15, for two AP/HTPB composite propellants (P1 and P2) and two alumina droplet diameters ( $1 \mu\text{m}$  and  $10 \mu\text{m}$ ). The propellant P1 contains micro-sized aluminum particles with a mass mean diameter of  $6 \mu\text{m}$  and the propellant P2 contains 20% of micro-sized aluminum particles (mass mean diameter of  $6 \mu\text{m}$ ) and 80% of nano-sized aluminum particles (mass mean diameter of  $100 \text{nm}$ ). The additional heat flux, due to radiation, influences burning rates and, consequently, the propellant ignition. Unsteady simulations of propellant ignition, with or without radiation, show in particular a significant

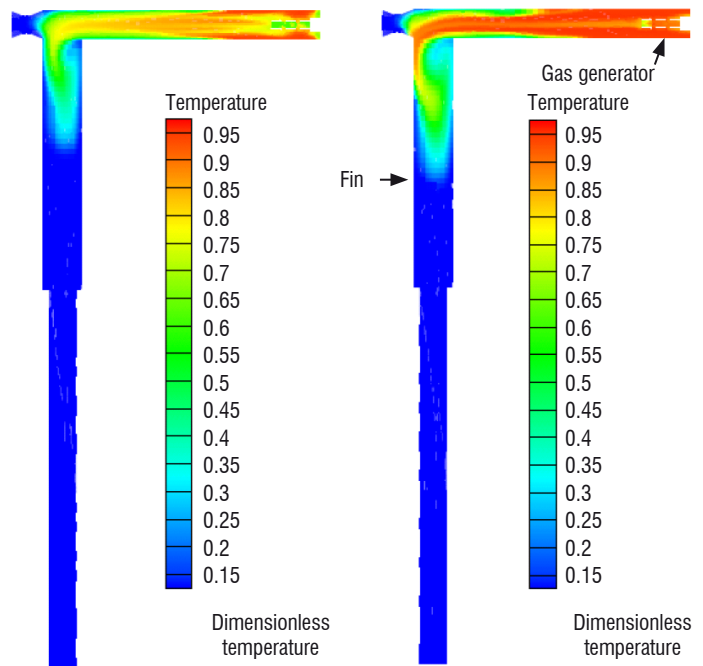


Figure 16 - Dimensionless temperatures, at a given time, obtained by simulations without (on the left) and with (on the right) taking into account radiative flux on the propellant surface.

role of radiative fluxes, as is shown in Figure 16. Dimensionless gas temperatures, obtained by simulations at the same physical time in an experimental setup studied at ONERA, are represented in this figure. This experimental facility consists of an igniter in a cylindrical gas generator and a perpendicular parallelepiped fin containing a test propellant to study the flame-spreading. As expected, Figure 16 shows that the propellant ignition is faster in the gas generator in which radiative flux is accounted for. The flame spread time in the fin is then modified.

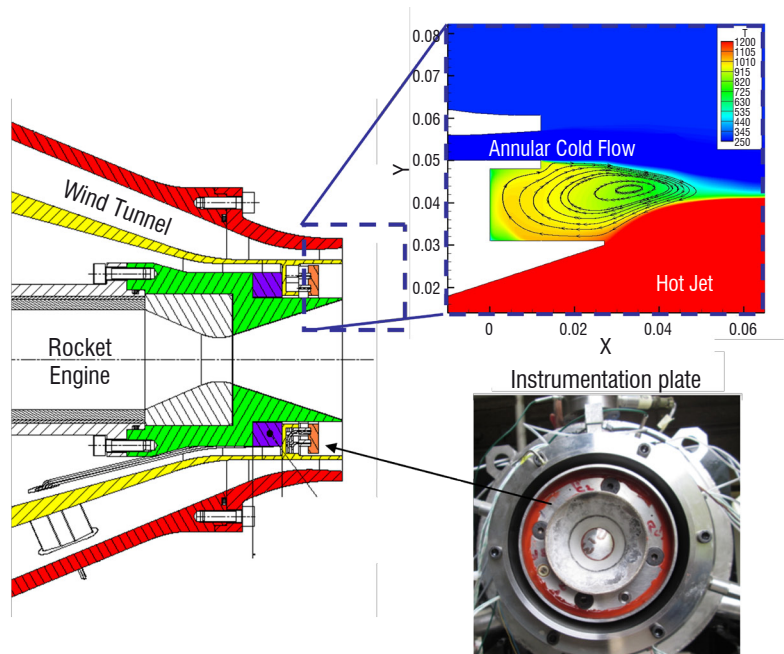


Figure 17 - The LP13 firing test facility consisting of a rocket motor jet surrounded by an annular cold air flow



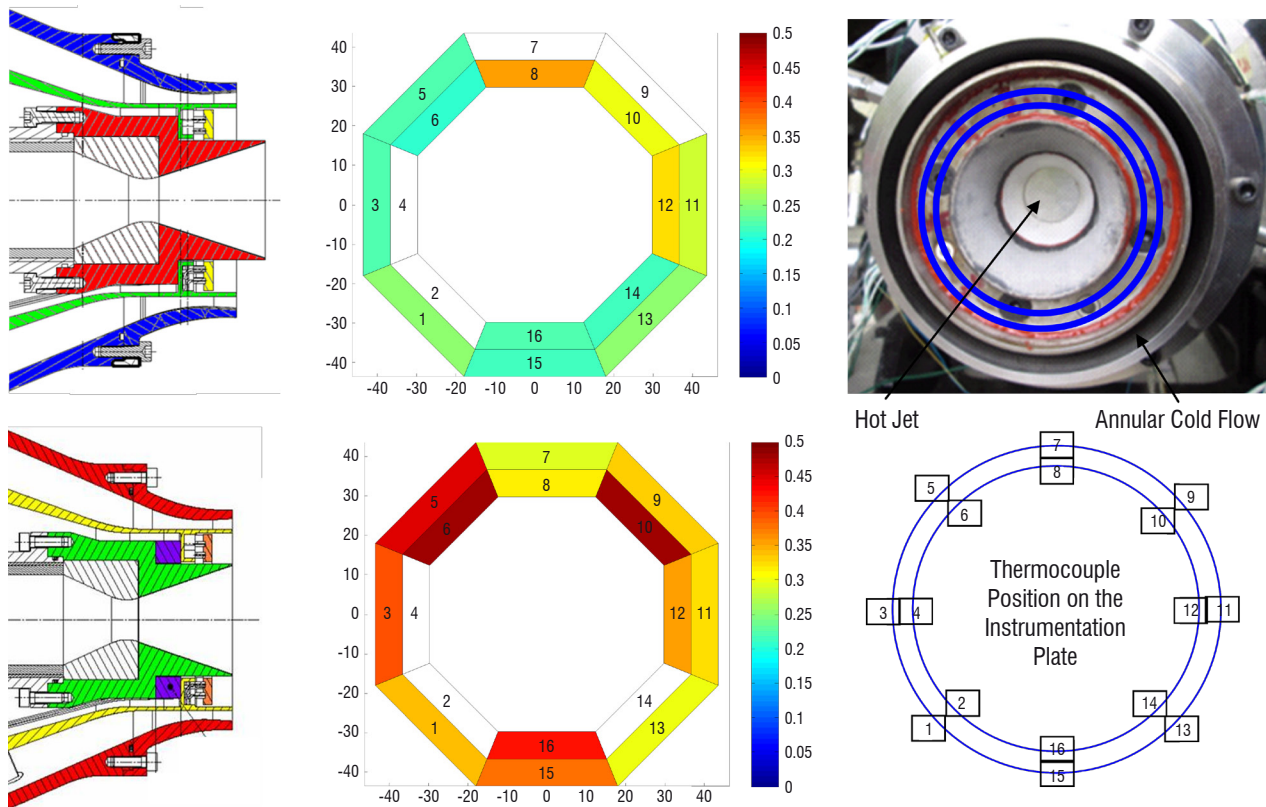


Figure 18 - Color representation of the heat flux level measured at different azimuthal positions in the base region between the hot jet and the annular cold air flow for two relative positions of the SRM with respect to the cold air flow nozzle

## Phenomena in the vicinity of the aft body

Flow separation is encountered in the vicinity of the aft body of a space launcher or a missile. Separated flows are highly unsteady and can introduce significant unsteady loads and loss of efficiency for a vehicle. The flow separation occurs because of a discontinuous variation in the aft body geometry and features strong oscillation of the propulsive system at transonic regime (buffeting). These phenomena are valid for both liquid rocket and solid rocket motors. In the latter case, a possible post-combustion of the propellant combustion gases with the ambient air may also occur in the exhaust jet. This post-combustion can be promoted by the presence of alumina particles in the recirculation zone induced by the separated flows around the nozzle. This induces very high heat fluxes in the vicinity of the aft body of the SRM, which needs to be taken into account in the design of the vehicle.

The flow conditions in the near wake of a vehicle propelled by a SRM are usually determined numerically. In order to validate these numerical tools, it is necessary to experimentally reproduce an external flow around the nozzle of a SRM, which required the development of a dedicated test bench. To be representative of the air flow environment in the aft body region of the motor, firing tests have to be performed inside a wind tunnel. The risks due to the pyrotechnic means, as well as the pollution of the wind tunnel due to the

emission of the combustion gases and particles, make this solution difficult to achieve. An alternative consists in designing a custom wind tunnel around a SRM.

The developed test bench, called the LP13 [51] firing test facility (Figure 17), consists of two parts, the motor and the wind tunnel. The motor is a downscaled SRM with a simplified geometry. The wind tunnel, being constructed around the motor, produces an annular cold flow around the hot jet of the SRM. The air flow capability ranges from subsonic to supersonic regimes. The test bench is highly instrumented throughout the air supply system, in the combustion chamber and in the aft body of the motor. Pressure, temperature and heat flux are measured at multiple points, especially in the base region.

Several firing tests have been performed by changing different parameters, such as the mass flow rate of the annular air flow and the relative position of the nozzle exit with respect to the cold flow nozzle exit. For instance, as indicated in Figure 18, the fact to back the position of the motor increases the heat flux in the aft body. The experimental database is used successfully to validate simulation results with the CEDRE code. The pressure and heat flux in the base region are well recovered by the simulation, which can predict the effect of the relative position of the two exits and the effect of the mass flow rate level.

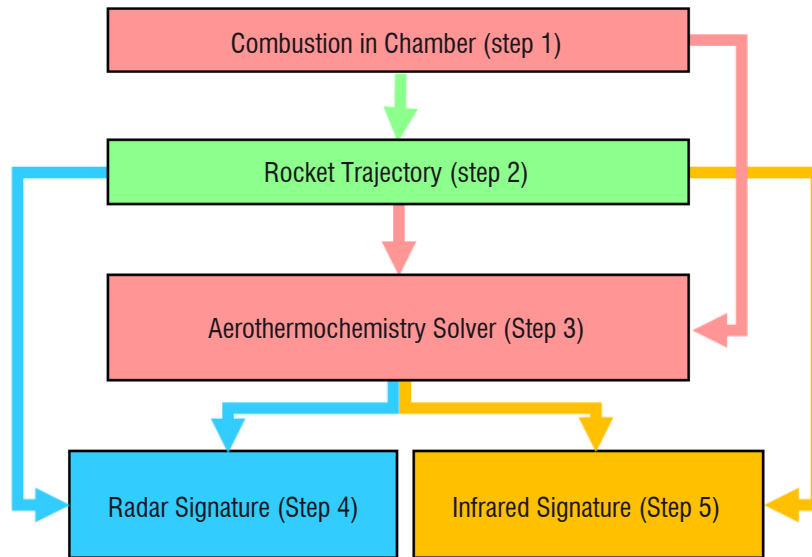


Figure 19 - The computation of plume signatures involves sequentially coupled multi-physics codes

## Solid rocket exhaust plumes

The study of rocket exhaust plumes is an exciting challenge for both numerical and experimental research. An exhaust plume is a supersonic afterburning flame, which appears in the mixing layer between combustion gases accelerated in the rocket nozzle and the atmosphere gases. With solid rocket motors with aluminized propellants, the flame is often visible to the naked eye, mainly because high-temperature alumina particles contained in the flow radiate in the visible part of the spectrum. Research on rocket plumes at ONERA most often finds its application in the prediction of infrared [52, 53] and radar signatures [54] of launchers or ballistic and tactical missiles. Other applications include the prediction of radiative and thermal transfers in the nozzle and aft regions of the rocket [55] or the study of pollutant diffusion in the atmosphere [56, 57]. In this section, we summarize recent developments in the research on signatures of rocket exhaust-plumes. We study these signatures with a dual approach, using both numerical simulations and comparison to measurements on small SRMs.

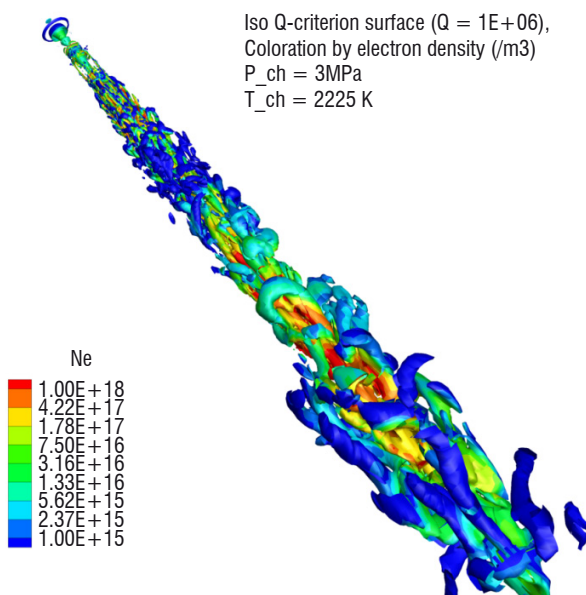


Figure 20 - Large eddy simulation of an ionized plume of a SRM. The isosurface of Q criterion is colored with the electron number density.

## Simulation platform

Our calculations of infrared and radar signatures of rocket plumes involve sequentially coupled multi-physics solvers, see Figure 19.

We calculate the composition of the burnt gas mixture (Step 1) in the rocket chamber using a chemical equilibrium code like STANJAN [58], or a rocket performance code like COPPELIA [59].

The rocket trajectory is then computed (Step 2) and the flight conditions are obtained at a given altitude. This information provides us with the necessary quantities to enforce the conditions on the boundaries of the computational domain for the plume flow simulation.

ONERA's CEDRE Platform [29] is used to simulate (Step 3) the supersonic gas flow in the plume. This solver performs calculations on unstructured meshes with cells of arbitrary geometry. We make use of a robust nonlinear Riemann solver for the treatment of shocks and rarefaction waves in the flow. The CEDRE solver also tracks alumina particles using Eulerian or Lagrangian approaches [30], with coupled interactions between particle dynamics and fluid flow. Turbulence creation and transport can be evaluated using a RANS model and a 2D-axisymmetric steady state solution is then obtained. Unsteady turbulent structures can also be computed using a 3D MILES approach, see Figure 20. A set of chemical reactions has been developed to describe the afterburning flame. This system involves 12 species ( $O$ ,  $O_2$ ,  $H$ ,  $H_2$ ,  $CO$ ,  $CO_2$ ,  $OH$ ,  $H_2O$ ,  $HCl$ ,  $Cl$ ,  $Cl_2$ ,  $N_2$ ), ionized species ( $K^+$ ,  $Na^+$ ,  $Cl^-$ ,  $e^-$ ) and 17 combustion reactions and additional ionization reactions whose rates are computed using a chemical kinetic mechanism developed at ONERA.

## Computation of signatures

In order to compute the static and dynamic radar signatures (Step 4) of the rocket plume, an ionization model has been developed [54] and integrated into the CEDRE code. In this model, we assume ambipolar diffusion for the ion and electron mixture in the plume. Electron number density and electron-neutral collision frequencies are used to compute the electric permittivity of the ionized plume. The radar signature of this non-homogeneous plasma is then computed by inverting the macroscopic Maxwell equations in the harmonic time domain.

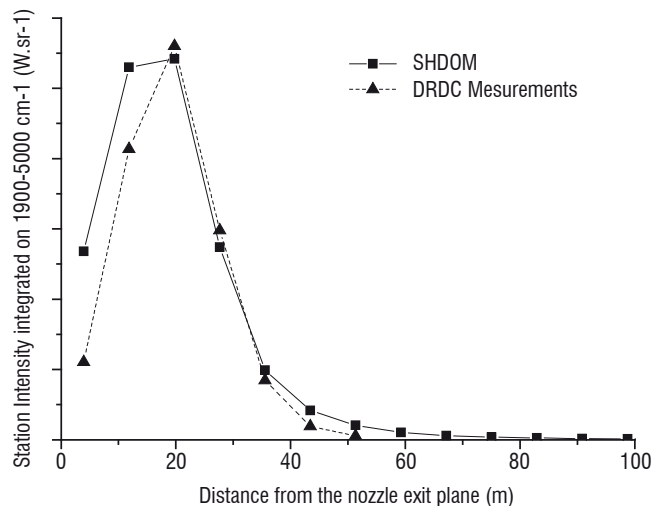
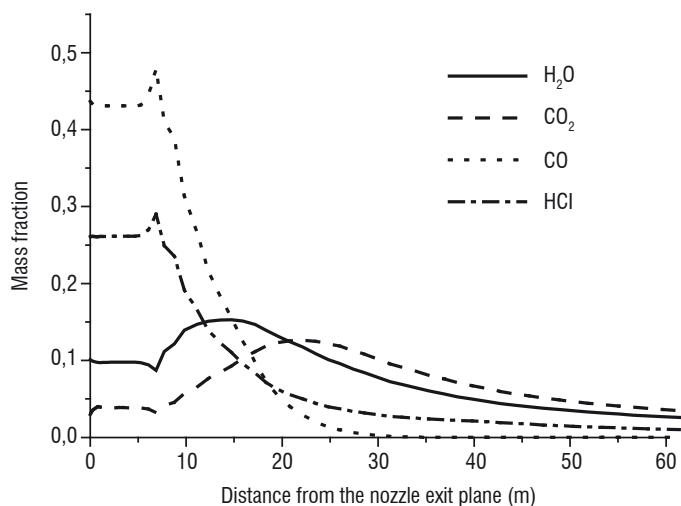


Figure 21 - Left: mass fraction of the radiating species computed by CEDRE along the center line of a Black Brant rocket at an altitude of 7.9 km  
Right: comparison between the computed and measured station radiation– spectral band 1900-5000 cm<sup>-1</sup>

The calculation of the plume infrared signature (Step 5) uses as input the plume temperature and pressure, the concentrations of the H<sub>2</sub>O, CO<sub>2</sub>, CO and HCl species and of the alumina particles computed with CEDRE, see Figure 21 (left). Radiative transfer computation is performed in a non-scattering medium, with either a line-by-line model or a statistical narrow-band model called RGM3000. The scattering media are dealt with by using the SHDOM solver [60]. We obtain good agreement between flight measurements and computations of the infrared signature of a Black Brant rocket [53], as shown in Figure 21 (right).

#### Ground firing of a solid rocket motor

In this paragraph, we shortly describe the experimental setup currently in use at ONERA to study the plume static and dynamic radar signatures. A small scale 2.5 kN thrust SRM is attached to the ground and fired during about 3 seconds. The ionization level in the chamber is controlled by adding 10 to 300 ppmw of potassium and sodium in the propellant, which itself originally contains traces (usually of the order of 10 ppmw) of such alkali metals. We make use of AP-HTPB propellant, with or without aluminum, the former leading to higher ionization levels in the plume. The backscattering of electromagnetic waves is studied using an UHF Doppler radar system, whose emitter

and receiver are shown in the background in Figure 22. The ionization level is strong enough for the radar system to record an energy spectrum with a Doppler shift between -4 kHz and 4 kHz. Further analysis of the Doppler signal is underway.

#### Conclusions and future work

We have developed numerical and experimental platforms to study solid rocket motor exhaust plumes. Our numerical platform makes use of a complex aerothermochemical solver and of a novel ionization model, which are sequentially coupled with infrared and electromagnetic codes to compute rocket plume signatures. We have been able to obtain a good comparison between the measured and simulated infrared signatures for rockets under real flight conditions. We have also recently begun to experimentally measure static and dynamic radar signatures underground conditions, and comparison with large eddy simulation results is underway. Future prospects include the modeling of exhaust plumes in a rarefied atmosphere to account for the high altitude of the rocket, with coupling between our Navier-Stokes solver and a DSMC (Dynamic Simulation Monte Carlo) code.

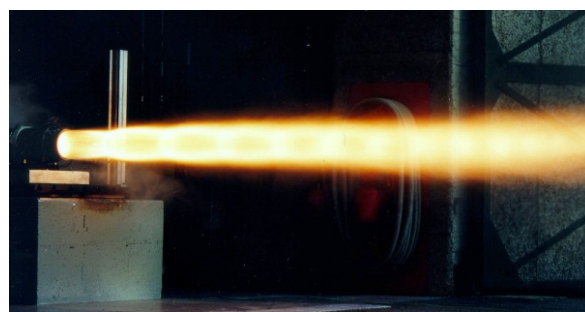
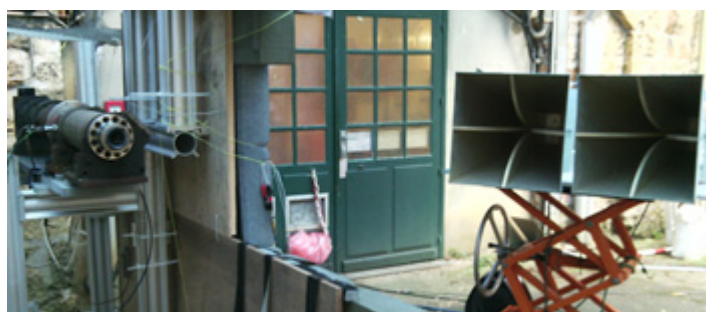


Figure 22 – Left: rocket nozzle to the left of the picture, radar emitter and receiver antennas in the background  
Right: exhaust plume during rocket firing.

## Conclusions and perspectives

The physical phenomena observed in a SRM chamber and in an exhaust plume are complex and involve interactions between chemistry, acoustics, turbulence, two-phase flows and radiative effects. Despite considerable experience accumulated by the industry in designing solid rocket motors for missiles, as well as space launchers, new developments require the physical phenomena to be more precisely understood, in order to guide the designer quickly towards less expensive and more reliable technical solutions. For this reason, research is being carried out in order to predict the behavior of solid rocket motors and their interaction with the atmosphere. This article

has allowed some physical phenomena currently studied at ONERA to be briefly described within the framework of several programs. CFD has become increasingly important and clearly brings new insights into solid rocket propulsion. However, well-instrumented experiments will always be necessary to validate numerical simulations or dedicated models.

In the near future, new projects will give us the opportunity to further investigate multi-physics and multi-scale phenomena in solid rocket propulsion, using parallel computing in order to analyze systems of ever increasing complexity ■

## Acknowledgements

This work has been done within the framework of several research programs supported by the DGA, the French Ministry of Defense, the CNES (*Centre National d'Études Spatiales*) and ONERA. The massively parallel simulations required for the turbulence study in a SRM have been performed on GENCI machines. The authors would like to thank the CINES. They also want to acknowledge valuable discussions with research engineers from SAFRAN/HERAKLES.

## References

- [1] Y. FABIGNON, J. DUPAYS, G. AVALON, F. VUILLOT, N. LUPOGLAZOFF, G. CASALIS, M. PRÉVOST - *Instabilities and Pressure Oscillations in Solid Rocket Motors*. Aerospace Science and Technology, Vol. 7, No. 3, 2003, pp. 191–200.
- [2] J. ANTHOINE - *Solid Propellant Pressure Oscillations*. VKI / STO-AVT-206 Lecture Series on Fluid Dynamics Associated to Launcher Developers, von Kármán Inst., Rhode-Saint-Genèse, Belgium, April 2013.
- [3] J. HIJLKEMA, M. PRÉVOST, G. CASALIS - *On the Importance of Reduced Scale Ariane 5 P230 Solid Rocket Motor Models in the Comprehension and Prevention of Thrust Oscillations*. CEAS Space Journal, Vol. 1, No. 4, 2011, pp. 99–107.
- [4] J. ANTHOINE, P. JÉZÉQUEL, P. PRÉVOT, M. PRÉVOST, G. CASALIS - *Variable Fuel Grains Burn Velocities to Reduce Solid-Rocket-Motor Pressure Oscillations*. Journal of Propulsion and Power, Vol. 31, No. 1, January-February 2015, pp. 342-351.
- [5] F. CHEDEVERGNE, G. CASALIS, T. FÉRAILLE - *Biglobal Linear Stability of the Flow Induced by Wall Injection*. Physics of Fluids, Vol. 18, January 2006.
- [6] G. BOYER, G. CASALIS, J-L. ESTIVALÈZES - *Stability and Sensitivity Analysis in a Simplified Solid Rocket Motor Flow*. Journal of Fluid Mechanics, vol. 722, pp. 618-644, 2013.
- [7] N. MEYNET - *Simulation numérique de la combustion d'un propergol solide*. Ph.D. Thesis, Université Paris VI, Paris 2005.
- [8] V. GIOVANGIGLI, N. MEYNET, M. SMOOKE - *Application of Continuation Techniques to Ammonium Perchlorate Plane Flames*. Combustion Theory and Modeling, Vol. 10, No. 5, 2006, pp. 771-798.
- [9] S. RAHMAN, V. GIOVANGIGLI, V. BORIE - *Pressure and Initial Temperature Sensitivity Coefficient Calculations in Ammonium Perchlorate Flames*. Journal of Propulsion and power, Vol. 27, No. 5, 2011, pp. 1054-1063.
- [10] B. NOVOZHILOV - *Theory of Nonsteady Burning and Combustion Stability of Solid Propellants by the Zel'dovich-Novozhilov Method*. Progress in Astronautics and Aeronautics, Vol. 143, chap. 15, 1992, pp. 601-641.
- [11] F.E.C. CULICK - *Unsteady Motions in Combustion Chambers for Propulsion Systems*. AGARDograph AG-AVT-309, RTO/NATO, Neuilly sur Seine, France, 2006.
- [12] J. FINLINSON, F. STALNAKER, F. BLOMSHIELD - *Ultra Pure Ammonium Perchlorate T-Burner Pressure Coupled Response at 500, 100 and 1800 psi*. 34th AIAA Joint Propulsion Conference, AIAA Paper 98-3554, July 1998.
- [13] V. GIOVANGIGLI, S. RAHMAN - *Numerical Simulation of Unsteady Planar Ammonium Perchlorate Flames Including Detailed Gas Phase Chemistry and Fluid-Structure Interaction*. Compte Rendu Académie des Sciences. Paris, C.R. Mécanique, 341, 152-160, 2013.
- [14] S. RAHMAN - *Modélisation et simulation numérique de flammes planes instationnaires de perchlorate d'ammonium*. Ph.D. Thesis, Université Paris VI, Paris 2012.
- [15] T.L. JACKSON - *Modeling of Heterogeneous Propellant Combustion: A Survey*. AIAA Journal, Vol. 50, No. 5, 2012, pp. 993-1006.
- [16] M. PLAUD, S. GALLIER, M. MOREL - *Simulations of Heterogeneous Propellant Combustion: Effect of Particle Orientation and Shape*. Proceedings of the Combustion Institute, Vol. 35, 2015, pp. 2447-2454.
- [17] M.L. GROSS, T.D. HEDMAN, S.F. SON, T.L. JACKSON, M.W. BECKSTEAD - *Coupling Micro and Meso-Scale Combustion Models of AP/HTPB Propellants*. Combustion and Flame, Vol. 160, 2013, pp. 982–992.
- [18] D. DAVIDENKO, Y. FABIGNON - *Some Aspects of Detailed Modeling of Solid Rocket Composite Propellants*. 6th EUCASS, Krakow, Poland, 29 June - 3 July 2015.
- [19] R.F. HOGLUND - *Recent Advances in Gas-Particle Nozzle Flows*. ARS Journal 32 (5), 1962, pp. 662-671.
- [20] R.W. HERMSEN - *Aluminum Oxide Particle Size for Solid Rocket Motor Performance Prediction*. AIAA paper 81-0035, AIAA 19th Aerospace Sciences Meeting, Jan. 12-15, 1981, St Louis, MO.
- [21] J. DUPAYS, Y. FABIGNON, P. VILLEDIEU, G. LAVERGNE, J.L. ESTIVALEZES - *Some Aspects of Two-Phase Flows in Solid-Propellant Rocket Motors*. Solid Propellant Chemistry, Combustion, and Motor Interior Ballistics, edited by V. Yang, T. B. Brill, and W.-Z. Ren, Vol. 185, Progress in Astronautics and Aeronautics, AIAA, Reston, 2000, pp. 859-883.

- [22] J. DUPAYS, F. GODFROY, O. ORLANDI, P. PRÉVOT, M. PRÉVOST, S. GALLIER, S. BALLEREAU, Y. FABIGNON - *Inert Condensed Phase Driving Effect of Combustion Instabilities in Solid Rocket Motor*. Space Propulsion 2008, May 5-9, 2008, Heraklion, Greece.
- [23] M.W. BECKSTEAD - *Evidences for Distributed Combustion*. Proceedings of the 24th JANNAF Combustion Meeting, CPIA Pub. 476, Vol. I, 1987, pp. 1-12.
- [24] S. GALLIER, F. GODFROY - *Aluminum Combustion Driven Instabilities in Solid Rocket Motors*. Journal of Propulsion and Power 25 (2) 509-521, 2009.
- [25] L. HESPEL, A. DELFOUR, B. GUILLAME - *Mie Light-Scattering Granulometer With an Adaptive Numerical Filtering Method*. II. Experiments. Applied Optics 40 (6) 974-985, 2001.
- [26] F. CAUTY, C. ERADES - *Tracking of Aluminum Particles Burning in Solid Propellant Combustion Gases by Focusing Schlieren Technique*. 15th International Symposium on Flow Visualization, Minsk, Belarus, June 25-28, 2012.
- [27] R. DEVILLERS, C. ERADES, D. LAMBERT, J. BELLESSA - *Mesure et suivi de particules, agglomérats et gouttes en combustion au-dessus de la surface d'un propergol en combustion*. 14ème Congrès Francophone de Techniques Laser, CFTL 2014, Marseille, 15-19 septembre 2014.
- [28] J. HIJKEMA, P. PRÉVOT - *Numerically-Assisted Particle Size Distribution Measurements in Reduce-Scale Solid Rocket Motors*. Journal of Propulsion and Power 31 (2) 714-724, 2015.
- [29] A. REFLOCH, B. COURBET, A. MURRONE, P. VILLEDIEU, C. LAURENT, P. GILBANK, J. TROYES, L. TESSÉ, G. CHAINERAY, J.B. DARGAUD, E. QUÉMERAIS, F. VUILLOT - *CEDRE Software*. Aerospace Lab, vol. 2, 2011.
- [30] A. MURRONE, P. VILLEDIEU - *Numerical Modeling of Dispersed Two-Phase Flows*. Aerospace Lab Journal AL02-04, pp. 1-13, 2011, <http://www.aerospacelab-journal.org/al2>.
- [31] F. DOISNEAU - *Eulerian Modeling and Simulation of Polydisperse Moderately Dense Coalescing Spray Flows with Nanometric-to-Inertial Droplets: Application to Solid Rocket Motors*. Ecole Centrale Paris thesis, 2013.
- [32] F. DOISNEAU, F. LAURENT, A. MURRONE, J. DUPAYS, M. MASSOT - *Eulerian Multi-Fluid Models for the Simulation of Dynamics and Coalescence of Particles in Solid Propellant Combustion*. Journal of Computational Physics 234, pp. 230-262, 2013.
- [33] R.A. BEDDINI - *Injection-Induced Flows in Porous-Walled Ducts*. AIAA Journal, Vol. 24, No. 11, 1986, pp. 1766-1773.
- [34] B. GAZANION, F. CHEDEVERGNE, G. CASALIS - *On the Laminar-Turbulent Transition in Injection-Driven Porous Chambers*. Experiments in Fluids, 55:1643, 2014.
- [35] F. VUILLOT - *Vortex Shedding Phenomena in Solid Rocket Motors*. Journal of propulsion and power 11 (4), 627-639, 1995.
- [36] J. DUPAYS - *Contribution à l'étude du rôle de la phase condensée dans la stabilité d'un propulseur solide pour lanceur spatial*. Ph.D. Thesis, INPT, 1996.
- [37] F. VUILLOT, N. LUPOGLAZOFF - *Comparison Between Firing Tests and Numerical Simulation of Vortex Shedding in a 2D Test Solid Motor*. AIAA paper 93-3066, AIAA 24th Fluid Dynamics Conference, Orlando, Florida, USA, July 1993.
- [38] F. VUILLOT, N. LUPOGLAZOFF - *Combustion and Turbulent Flow Effects in 2D Unsteady Navier-Stokes Simulations of Oscillatory Rocket Motors*. AIAA paper 96-0884, AIAA 34th Aerospace Sciences Meeting, Reno, Nevada, USA, Jan. 1996.
- [39] R. DUVAL - *Transferts radiatifs dans les moteurs à propergol solide*. Ph.D. Thesis, École Centrale Paris, 2002.
- [40] Y. JOUMANI - *Transferts radiatifs dans les moteurs à propergol solide*. Ph.D. Thesis, Université de Valenciennes et du Hainaut Cambresis, 2001.
- [41] L. TESSÉ, J.-M. LAMET - *Radiative Transfer Modeling Developed at Onera for Numerical Simulations of Reactive Flows*. AerospaceLab Journal, Issue 2, March 2011, <http://www.aerospacelab-journal.org/al2>.
- [42] F. DUPOIRIEUX, L. TESSÉ, A. AVILA J. TAINE - *An Optimized Reciprocity Monte Carlo Method for the Calculation of Radiative Transfer in Media of Various Optical Thicknesses*. International Journal of Heat and Mass Transfer, Vol. 49, pp. 1310-1319, 2006.
- [43] L. TESSÉ - *Modélisation des transferts radiatifs dans les flammes turbulentes par une méthode de Monte Carlo*. Ph.D. Thesis n°2001-34, École Centrale de Paris, 2001.
- [44] L. TESSÉ, F. DUPOIRIEUX, B. ZAMUNER, J. TAINE - *Radiative Transfer in Real Gases Using Reciprocal and Forward Monte Carlo Methods and a Correlated-k Approach*. International Journal of Heat and Mass Transfer, Vol. 45, pp. 2797-2814, 2002.
- [45] L. TESSÉ, F. DUPOIRIEUX, J. TAINE - *Monte Carlo Modeling of Radiative Transfer in a Turbulent Sooty Flame*. International Journal of Heat and Mass Transfer, Vol. 47, pp. 555-572, 2004.
- [46] O. ROUZAUD, L. TESSÉ, T. SOUBRIÉ, A. SOUFIANI, PH. RIVIÈRE, D. ZEITOUN - *Influence of Radiative Heating on a Martian Orbiter*. Journal of Thermophysics and Heat Transfer, Vol. 22, No. 1, pp. 10-19, January-March 2008.
- [47] R. DUVAL, A. SOUFIANI, J. TAINE - *Coupled Radiation and Turbulent Multiphase Flow in an Aluminized Solid Propellant Rocket Engine*. Journal of Quantitative Spectroscopy and Radiative Transfer, Vol. 84, pp. 513-526, 2004.
- [48] PH. RIVIÈRE, A. SOUFIANI - *Updated Band Model Parameters for H<sub>2</sub>O, CO<sub>2</sub>, CH<sub>4</sub> and CO Radiation at High Temperature*. International Journal of Heat and Mass Transfer, Vol. 55, pp. 3349-3358, 2012.
- [49] L. A. DOMBROVSKY - *Possibility of Determining the Disperse Composition of a Two-Phase Flow from the Small-Angle Light Scattering*. High Temperature, Vol. 20, pp.472-479, 1982.
- [50] J.M. LAMET, Y. FABIGNON, L. TESSÉ, J. DUPAYS, E. RADENAC - *Modeling of Propellant Combustion with Nano-Sized Aluminum Particles*. Proceedings of the 5th European Conference for AeroSpace Sciences (EUCASS 2013), Munich, Allemagne, 1-5 juillet 2013.
- [51] L. PASCAL, P. PRÉVOT, P. REULET, J. DUPAYS, J. ANTHOINE - *Development of a Test Facility for Investigating the Solid Rocket Motor Base Region in Representative External Flow Conditions*. To be presented at Space Propulsion 2016, Roma, Italy, 2-6 May 2016.
- [52] A. BOISCHOT, A. ROBLIN, L. HESPEL, I. DUBOIS, P. PREVOT, T. SMITHSON - *Evaluation of Computation Codes for Rocket Plume's Infrared Signature by Using Measurements on a Small Scale Aluminized Composite Propellant Motor*. Proceedings of SPIE - The International Society for Optical Engineering, 17-18 April, 2006, Kissimmee, Florida, USA.
- [53] V. RIALLAND, A. GUY, D. GUEYFFIER, P. PEREZ, A. ROBLIN, T. SMITHSON - *Infrared Signature Modeling of a Rocket Jet Plume - Comparison with Flight Measurements*. Journal of Physics: Conference Series, in press.
- [54] D. GUEYFFIER, B. FROMENTIN-DENOZIERE, J. SIMON, A. MERLEN, V. GIOVANGIGLI - *Numerical Simulation of Ionized Rocket Plumes*. Journal of Thermophysics and Heat Transfer, 2014, Vol. 28:2, pp. 218-225.

- [55] J.B. DARGAUD, J. TROYES, J.M. LAMET, L. TESSÉ, F. VUILLOT, C. BAILLY - *Numerical Study of Solid-Rocket Motor Ignition Overpressure Wave Including Infrared Radiation*. Journal of Propulsion and Power, 30(1), pp. 164-174, 2013.
- [56] A.D. KOCH, C. BAUER, E. DUMONT, F. MINUTOLO, M. SIPPEL, P. GRECARD, G. ORDONNEAU, H. WINKLER, L. GUÉNOT, C. LINCK, C. R. WOOD, J. VIRA, M. SOFIEV, V. TARVAINEN - *Multidisciplinary Approach for Assessing the Atmospheric Impact of Launchers*. 4th CEAS Air & Space Conference, 2013.
- [57] A. POUBEAU - *Simulation des émissions d'un moteur à propergol solide: vers une modélisation multi-échelle de l'impact atmosphérique des lanceurs*. Ph.D. Thesis, Université de Toulouse, Université Toulouse III-Paul Sabatier, 2015.
- [58] W. C. REYNOLDS - *The Element Potential Method for Chemical Equilibrium Analysis: Implementation in the Interactive Program STANJAN*. Department of Mechanical Engineering, Stanford University, 1986.
- [59] B. BOURASSEAU - *Code COPPELIA: version 3.0. Calcul de la composition de produits de combustion contenant de nombreuses phases condensées*. ONERA Report, RT 40/4386 DEFA/N.
- [60] J.B. PAUTRIZEL, A. ROBLIN, P. PEREZ, V. RIALLAND - *Absorption-Scattering Coupling for the Infrared Signature of an Aluminized Solid Rocket Motor*. Proceedings of the 6th International Symposium on Radiative Transfer, Antalya, Turkey, 13-19 June 2010.

#### List of acronyms

AP	(Ammonium Perchlorate)
ARM	(Absorption Reciprocity (Monte Carlo) Method)
CEDRE	( <i>Calcul d'Écoulements Diphasiques Réactifs pour l'Energétique</i> )
CFD	(Computational Fluid Dynamics)
CINES	( <i>Centre Informatique National de l'Enseignement Supérieur</i> )
CPU	(Central Processing Unit)
DNS	(Direct Numerical Simulation)
DOM	(Discrete Ordinates Method)
ERM	(Emission Reciprocity (Monte Carlo) Method)
FM	(Forward (Monte Carlo) Method)
GENCI	( <i>Grand Equipement National de Calcul Intensif</i> )
HPC	(High Performance Computing)
HTPB	(Hydroxyl-Terminated PolyButadiene)
KeRc	(Keldysh Research center)
LES	(Large Eddy Simulation)
MCM	(Monte Carlo Method)
MILES	(Monotonically Integrated Large Eddy Simulation)
ORM	(Optimized Reciprocity (Monte Carlo) Method)
RANS	(Reynolds-Averaged Navier Stokes (equations))
RSA	(Random Sequential Adsorption)
RTE	(Radiative Transfer Equation)
SNB	(Statistical Narrow-Band)
SRM	(Solid Rocket Motor)
ZN	(Zel'dovich-Novozhilov (response function))



**Yves Fabignon** is currently the Head of the Solid Propulsion Unit of the Fundamental and Applied Energetics Department (DEFA) at ONERA. He obtained a Ph.D. in Energetics from the University of Poitiers, ENSMA in 1984. He worked previously for 8 years at the SNPE (now SAFRAN/HERAKLES) before joining ONERA.



**Jérôme Anthoine** is currently the Head of the Propulsion Laboratory Unit of the Aerodynamics and Energetics Modeling Department (DMAE) at ONERA. He received the Mechanical Engineering Degree from the *Faculté Polytechnique de Mons* (Belgium) in 1995 and the von Karman Institute Diploma in 1996. Then, he obtained a Ph.D. in Space Propulsion from the *Université Libre de Bruxelles* (Belgium) in 2000. At that time, he joined the Faculty of the von Karman Institute as Assistant Professor and then Associate Professor, to develop the aeroacoustics and space propulsion activities. Since 2009, he joined ONERA as senior scientist in Space Propulsion and is currently managing research activities on pressure oscillations in solid rocket motors and on hybrid chemical propulsion.



**Dmitry Davidenko** is currently a senior research engineer specialized in the rocket propulsion area. He obtained a PhD in Mechanics and Energetics from the University of Orléans. He has been working at ONERA since 2011. Dmitry's principal activities are in the field of detailed modeling of composite solid propellant combustion. He also participates in projects on simulation of complex reacting flows in solid rocket motors. Another activity concerns numerical studies on the use of rotating detonation for rocket propulsion.



**Robin Devillers** has been a research engineer at ONERA since 2013. He is in charge of experimental measurements associated with solid propellant studies, ranging from material characterization to combustion imaging. He worked previously for 4 years at the National Research Center of Canada in Ottawa on optical diagnostics for soot emission characterization in gas flares, with measurement campaigns performed in oil refineries in Mexico. He obtained his PhD from *École Centrale Paris* for his work on laser techniques for temperature measurements in engines at IFP. He has a MSc and an engineering degree from *École Centrale Paris*.



**Joël Dupays** is currently a senior scientist and project manager at ONERA. Specialized in the solid propulsion area, his research activity combines fluid dynamics and energetics with a special focus on droplet combustion and unsteady polydisperse two-phase flow modeling and simulation. He received a PhD in Fluid Mechanics from the National Polytechnic Institute of Toulouse in 1996.



**Denis Gueyffier** is currently a senior scientist at ONERA. He performs research on numerical simulation of solid rocket propulsion and manages projects with government agencies and industrial customers. He was previously a researcher at NASA Goddard Institute of Space Studies in NYC, in the climate modeling team. As a Research Scientist at the Courant Institute in NYC, he contributed to the design of fast algorithms accelerating by orders of magnitude molecular electrostatics and fluid dynamics computations. He was also an Instructor of Applied Mathematics at MIT, where he did research on numerical simulation of multiphase flows. He obtained a PhD from the University of Paris VI in the field of Fluid Mechanics with a fellowship from the French Space Agency.



**Jouke Hijlkema** is a senior scientist at ONERA. He performs research in the domain of rocket propulsion and manages projects with government agencies and industrial customers. He received a masters degree in aeronautical engineering from *Hogeschool Haarlem* and a masters degree in mathematics from the university of Nijmegen, both in the Netherlands. He obtained a PhD from ISAE in Toulouse, in the field of applied mathematics.



**Nicolas Lupoglazoff** is a senior scientist, graduated from the "*École Nationale Supérieure de l'Aeronautique et de l'Espace*" in 1987. He joined ONERA's Energetics Department in 1988, and is now in the Fundamental and Applied Energetics Department. He is working in the field of CFD and is specialized in aerodynamics and acoustics in engine nozzles and jets. He is also working on the numerical simulation of the instabilities and turbulence inside solid rocket motors.



**Lionel Tessé** received his Ph.D. degree, in energetics and the physics of transfer, from the *École Centrale Paris* in 2001. For his Ph.D., he worked on the modeling, using the Monte Carlo method, of radiative transfer in a turbulent sooty flame, focusing on the interaction between turbulence and radiation. He has been a research scientist at ONERA, in the Applied and Fundamental Energetics Department, since 2001. His research topics include the modeling and simulation of radiative transfer in aeroengine combustors, solid propellant rocket motors and hypersonic flows occurring during atmospheric (re-)entries. He is in charge of the development of the ASTRE code (Monte Carlo) and is involved in the development of the REA code (DOM), both codes dedicated to radiative transfer computations.



**Jean-Michel Lamet** graduated from the *École Nationale Supérieure d'Ingénieurs* de Poitiers in 2005 and received his Ph.D. degree from *École Centrale Paris* in 2009. For his Ph.D., he worked on the radiative transfer in atmospheric re-entry hypersonic flows. He now holds a position of research scientist in the ONERA Applied and Fundamental Energetics Department. His activity includes the modeling and simulation of radiative transfer in combustion chambers and hypersonic flows. He is involved in the development of the ASTRE and REA codes dedicated to radiative transfer.



**Aurélien Guy** has been a junior research engineer at ONERA since 2014. His activities are focused on exhaust plume modeling and numerical simulation for application, including optical and electromagnetic signature prediction. He obtained a PhD from the Em2c laboratory at the *École Centrale Paris* in 2013 in the field of energetics, working on the thermochemical modeling and simulation of shock waves for atmospheric reentry using collisional-radiative models.



**Charles Erades**, Aerospace engineer, has been working at ONERA in the Fundamental and Applied Energetics Department for the past 30 years. He has developed experimental setups for the characterization of solid propellants and internal thermal protections for rocket motors. He is specialized in non-intrusive ultrasonic methods for the evaluation of pyrolysis and burning rates. He has also worked on characterizing aluminum-droplet burning time with the optical diagnostics that he developed. Furthermore, he implemented experimental motor-jet studies and investigated burning instabilities, as well as studying propellant-ignition delays.